Superionic and Metallic States of Water and Ammonia at Giant Planet Conditions

C. Cavazzoni, G. L. Chiarotti,* S. Scandolo, E. Tosatti, M. Bernasconi, M. Parrinello

The phase diagrams of water and ammonia were determined by constant pressure ab initio molecular dynamic simulations at pressures (30 to 300 gigapascal) and temperatures (300 to 7000 kelvin) of relevance for the middle ice layers of the giant planets Neptune and Uranus. Along the planetary isentrope water and ammonia behave as fully dissociated ionic, electronically insulating fluid phases, which turn metallic at temperatures exceeding 7000 kelvin for water and 5500 kelvin for ammonia. At lower temperatures, the phase diagrams of water and ammonia exhibit a superionic solid phase between the solid and the ionic liquid. These simulations improve our understanding of the properties of the middle ice layers of Neptune and Uranus.

Density profiles of Uranus and Neptune suggest that, buried between a rocky core and a gaseous atmosphere, their interiors are composed mostly of a thick intermediate layer of "hot ices," predominantly water, hydrocarbons, and ammonia in solar proportions (molar fractions: 56% H_2O, 36% CH_4, and 8% NH_3) (*1*). Pressure and temperature conditions within the ice layer range from 20 GPa and 2000 K to 600 GPa and 7000 K (*2*) along the planetary isentrope. Many observable properties of these planets, such as gravitational moment and atmospheric composition, are thought to be determined by the physical and chemical properties of matter within this layer. In particular, the ice layer is considered to be the source of the magnetic fields measured by the Voyager 2 spacecraft at Uranus and Neptune (*3*). Electrical conductivities in the ice layer on the order of 10 ohm^{-1} cm^{-1} are necessary to sustain the planetary dynamo mechanism for the generation of such a magnetic field (*4*). Because water is the most abundant component of the mixture, it has been suggested (*4*, *5*) that the large conductivity may arise from nearly complete ionization of H_2O. However, water metallization cannot be ruled out at the extreme conditions of the deeper regions of the ice layer. If this is the case, electronic conduction may also contribute to the dynamo (*6*).

The only nonastronomical data available on the behavior of ices at these extreme conditions come from shock-wave experiments. The equation of state (EOS) of water and ammonia and of a mixture of water, ammonia, and isopropanol termed "synthetic Uranus" have been measured in shock-wave experiments up to 200 GPa (*5*, *7*). The shock-wave measurements provide constraints on the density profiles of Uranus and Neptune (*8*) and show that the electrical conductivity in water and ammonia increase exponentially along the Hugoniot up to ~20 GPa and then levels off (*5*, *7*). These data are consistent with activated molecular dissociation at low pressure, whereas the high-pressure plateau suggests a nearly constant concentration of dissociated species. The measured value of the conductivity of water above 20 GPa (10 ohm^{-1} cm^{-1}) supports the planetary dynamo models. However, the absence of conductivity data for water and ammonia above 77 GPa and the uncertainty about the conduction mechanisms limit the development of models for the origin of the magnetic fields of Neptune and Uranus.

Computer simulations can explore regions of the phase diagram not directly accessible by experiments. Ab initio methods are essential for describing hydrogen bonding and molecular dissociation in water and ammonia. In the past ab initio simulations allowed us to determine the high-pressure, high-temperature behavior of methane, one of the components of the ice layer (*9*), and the structural phase transitions of ice at high pressure (*10*, *11*). In particular, from simulations at 300 to 400 GPa a new crystalline phase of ice was found and was predicted to display fast proton conductivity above 2000 K (*11*). The finding of a fast ionic conductor phase of ice agrees with earlier proposals (*12*) and provides support for the ionic model of the conductivity in the ice layer. However, compelling theoretical support for this model requires a full and precise determination of the phase diagram of ices along the planet's isentrope.

Here we report on ab initio molecular dynamic simulations (*13*) aimed at estimating the phase diagram of water and ammonia at pressures and temperatures in the range 30 to 300 GPa and 300 to 7000 K. The simulations also yield the EOS (pressure versus density) of water and ammonia which, complemented by that already available for methane (*9*), are needed for calculation of the radial density distributions for comparison with those derived from the gravitational field measured by spacecraft. Moreover, the simulations can provide values of the electrical conductivity needed for the calculation of the magnetic field generated by the planetary dynamo (*14*). Constant pressure deformable cell simulations (*15*) were conducted on supercells containing 32 water molecules or 64 ammonia molecules, with periodic boundary conditions at 30, 60, 150, and 300 GPa (*16*). The temperature was, for each pressure, increased from 300 to 7000 K in steps of 500 K. Simulation runs were 1 to 3 ps long, at fixed pressure and temperature.

For water, the low-temperature starting configurations were chosen to be the ice VII structure at 30 and 60 GPa (*17*) and the ice X structure at 150 and 300 GPa (*18*). In ice VII and ice X the oxygen atoms form a body-centered cubic (bcc) sublattice. The two phases differ only in the position of the protons, which are off-center in ice VII and at the center of the O-O separation in ice X. The phase diagram of water that we derived from the simulations is shown in Fig. 1A.

By increasing the temperature we found that at all the pressures we considered, an abrupt transition occurred at ~2000 K, after which the protons become highly diffusive (diffusion coefficient D_H^{water}(150 GPa, 2500 K) = 6 (±1) × 10^{-4} cm^2/s). Diffusion occurs by jumps among equivalent sites along the O-O separations. At this temperature the simulation shows that the oxygen atoms still vibrate around the bcc lattice positions, leading to a superionic solid phase of space group $Pn\bar{3}m$. A further increase in temperature ($T > 3500$ K) leads to the melting of the oxygen sublattice [D_O^{water} (150 GPa, 4000 K) = 3 (± 1.5) × 10^{-5} cm^2/s] and to an increase in the proton mobility [D_H^{water} (150 GPa, 4000 K) = 1.8 (±0.3) × 10^{-3} cm^2/s], indicating a further transition to a fluid phase.

To determine whether the proposed crystallinity of the oxygen sublattice observed below 3000 K was due to a well-defined superionic solid or was an artifact of the short simulation times, we examined the caloric curve $E(T)$ (where E is the internal energy), which was found to exhibit two well-defined

C. Cavazzoni, G. L. Chiarotti, S. Scandolo, Istituto Nazionale per la Fisica della Materia (INFM) and International School for Advanced Studies (SISSA), Via Beirut 4, I-34014 Trieste, Italy. E. Tosatti, INFM and SISSA, Via Beirut 4, I-34014 Trieste, Italy, and International Centre for Theoretical Physics (ICTP), I-34014 Trieste, Italy. M. Bernasconi, INFM, and Dipartimento di Scienza dei Materiali, Universitá di Milano, Via Emanueli 15, I-20126 Milan, Italy. M. Parrinello, Max-Planck- Institut für Festkörperforschung, Heisenbergstr. 1, D-70569 Stuttgart, Germany.

*To whom correspondence should be addressed. E-mail: guido@sissa.it

jumps of $\Delta E = 0.4$ eV per molecule at the solid-to-superionic solid transition and $\Delta E = 0.8$ eV per molecule at the superionic solid-to-liquid transition. Moreover, crystallinity of the superionic phase remains stable even in the presence of a H_2O vacancy. Finally, the ionic liquid phase is found to freeze spontaneously when cooled in the superionic solid temperature region. The oxygens solidify in an amorphous state, whereas the protons are still highly diffusing. This amorphous phase, moreover, is found to melt at about 500 K (at 150 GPa) below the corresponding ordered superionic solid melting temperature. We thus conclude that a well-defined superionic crystalline phase is present in the phase diagram of water.

The fluid observed above 3500 K is dissociated and resembles a two-component ionic liquid (molten salt). The same behavior is observed by decreasing the pressure to 30 GPa in the fluid phase. This confirms the experimental findings that locate the cross-over from ionic to molecular liquid at a somewhat lower pressure (~20 GPa) (*5*). The superionic solid state and the ionic liquid state have an electronically insulating character. The electronic density of states at 300 GPa shows that the electronic gap decreases from 10 eV at 300 K to about 5 eV at 2500 K, within the superionic phase, and finally closes at about 7000 K, inside the fluid phase. At lower pressures (150 GPa) metallization is observed at a higher temperature of 7500 K.

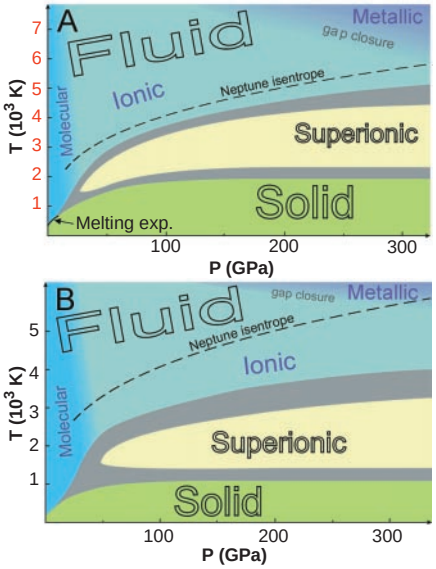

Fig. 1. Phase diagram of (**A**) water and (**B**) ammonia as determined from the ab initio simulations. The gray regions indicate the error bar on the predicted phase boundaries (*21*). The Neptune isentrope (dashed line) is taken from (*2*). For (A), because of the presence of the superionic phase, the melting curve of water at high pressure is reached at higher temperatures than predicted by extrapolating low-pressure experimental data (solid line) (*32*).

The computed phase diagram for ammonia (Fig. 1B) is similar to the computed phase diagram for water. The superionic solid, the nonmetallic ionic liquid, and the metallic ionic liquid states are all present in ammonia, but they set in at lower temperatures compared to water. In the simulation, we found that the pseudo–hexagonal close-packed (hcp) ($P2_12_12_1$) crystalline structure of ammonia is stable at low temperature in the range 5 to 15 GPa, in agreement with experiments (*19*). No phase transitions or hydrogen-bond symmetrization takes place by increasing the pressure up to 300 GPa in the 300 K simulations. We observed only that the small distortion of the nitrogen sublattice from ideal hcp decreases continuously with increasing pressure. On the other hand, by fixing the pressure at 30 GPa and increasing the temperature we found a transition from solid to molecular liquid by an intermediate plastic phase setting in at 600 K. By increasing the pressure in the fluid a cross-over from a molecular liquid to an ionic state was found (Fig. 1B). Starting from the same $P2_12_12_1$ configuration but increasing temperature at a higher pressure (≥60 GPa) we observed, in place of the solid–molecular fluid transition, a transition from the $P2_12_12_1$ structure to an hcp superionic solid above 1200 K. A triple point is thus present in the phase diagram between 30 and 60 GPa. In the superionic phase the protons jump between neighboring molecules. Each molecule still has three protons at any given time (which implies that proton jumps are highly correlated), but the angular distribution of protons around each nitrogen does not show any preferential direction. This is in contrast with superionic water, where the protons are located near the O-O bond centers, between one hopping event and the next. The proton diffusion coefficient in the superionic phase of ammonia is similar to that of water, $D_H^{ammonia} = 3\ (\pm 0.4) \times 10^{-4}$ cm²/s at 2000 K and 150 GPa. Also, at 300 GPa, ammonia metallizes at ~5500 K.

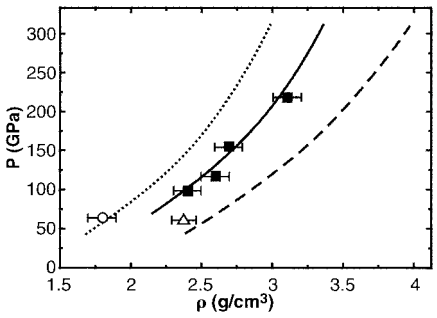

Fig. 2. Pressure versus density curves along the planetary isentrope of Fig. 1. Our results for ammonia (dotted line) and water (dashed line) are compared with shock-wave data for ammonia (○) (*7*) and water (△) (*33*). The discrepancy in water at 60 GPa is attributable to the fact that the shock-wave temperature was 4300 K, while the simulation was carried out at 3000 K (*34*). Shock-wave data of "synthetic Uranus" (■) [(*5*), see text] are compared with the EOS obtained from simulations of methane (*9*), ammonia, and water and by using the additive volumes law (*20*).

The computed EOSs of water and ammonia close to the planetary isentrope can be compared with shock wave data (Fig. 2). By using the additive volume law (*20*) we estimated the pressure versus volume curve of the mixture of water, ammonia, and methane at solar proportions. The results agree with shock wave data available for "synthetic Uranus" and provide an estimate of the EOS of the ices mixture at higher pressure and temperature.

The above results enhance our understanding of the properties of the middle ice layers of Uranus and Neptune. The precise location of the planetary isentrope (Fig. 1) is subject to large uncertainties depending on the model of the planet's interior that is chosen. Within the uncertainties of our simulations (*21*), we find that the melting curves of water and ammonia run below all the presently accepted planetary isentropes (*2*, *22*) (Fig. 1), confirming that in the middle layer planetary ices are in the fluid state. Within the fluid phase three distinct behaviors have been observed: (i) a molecular regime at low pressure, (ii) a nonmetallic ionic regime at intermediate pressure and temperature, and (iii) a metallic regime at high pressure and temperature. Along the planetary isentrope ammonia and water components of the ice layer are predicted to be electronically insulating up to 300 GPa. Thus, the electrical conductivity in the outer part of the ice layers can come only from the large proton mobility in the ionic liquid phase. Our computed ionic conductivity (*23*) agrees with shock-wave data measured up to 60 GPa (Fig. 3). Our results also provide an interpretation of the pressure dependence of the conductivity. At low pressures molecular water exhibits a low ionic conductivity arising from dissociated mole-

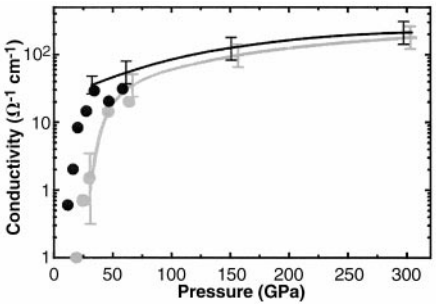

Fig. 3. Ionic conductivity of water (black) and ammonia (gray) along the planetary isentrope of Fig. 1, as computed in the simulation (lines with error bars) and measured in shock-wave experiments (circles) (*7*, *33*).

cules. By increasing the pressure, the number of dissociated molecules (and thus of the protonic carriers) increase exponentially across the molecular-ionic cross-over. In the ionic regime all the protons contribute equally to the conductivity, and a further increase in pressure increases the proton mobility without changing the number of carriers.

Moving deeper into the planet, the ice core boundary is met at 600 GPa and 7000 K according to the presently accepted planetary isentrope (*2*). At these conditions we predict water and ammonia to be metallic (*24*). This may have at least two consequences. First, the dynamo generation of the magnetic field should include the contribution of the high electronic conductivity due to the metallic liquid in the inner part of the ice layer, and the lower electrical conductivity due to the proton mobility in the electronically insulating liquid in the outer part of the ice layer. Second, a metallic state of water may affect its solubility with hydrogen and rocks. This may alter current views on the partitioning of these materials in the deepest regions of the ice layer. However, alternative models of the giant planets have been proposed which assume that above 150 GPa the interior is isothermal at a temperature of ≈5000 K (*2*, *25*). In this case the ices will remain electronically insulating in the whole planet.

References and Notes

1. W. B. Hubbard, *Science* **214**, 145 (1981).
2. _____, M. Podolak, D. J. Stevenson, in *Neptune and Triton*, D. P. Cruikshank, Ed. (Univ. of Arizona Press, Tucson, AZ, 1995), pp. 109–138.
3. N. F. Ness *et al.*, *Science* **233**, 85 (1986); *ibid.* **246**, 1473 (1989).
4. R. L. Kirk and D. J. Stevenson, *Astrophys. J.* **316**, 836 (1987).
5. W. J. Nellis *et al.*, *Science* **240**, 779 (1988).
6. D. J. Stevenson, *Rep. Prog. Phys.* **46**, 555 (1983).
7. W. J. Nellis, N. C. Holmes, A. C. Mitchell, D. C. Hamilton, M. Nicol, *J. Chem. Phys.* **107**, 9096 (1997).
8. W. B. Hubbard *et al.*, *Science* **253**, 648 (1991).
9. F. Ancilotto, G. L. Chiarotti, S. Scandolo, E. Tosatti, *ibid.* **275**, 1288 (1997).
10. M. Benoit, D. Marx, M. Parrinello, *Nature* **392**, 258 (1998); M. Bernasconi, P. L. Silvestrelli, M. Parrinello, *Phys. Rev. Lett.* **81**, 1253 (1998).
11. M. Benoit, M. Bernasconi, P. Focher, M. Parrinello, *Phys. Rev. Lett.* **76**, 2934 (1996).
12. P. Demontis, R. L. LeSar, M. L. Klein, *ibid.* **60**, 2284 (1988).
13. R. Car and M. Parrinello, *ibid.* **55**, 2471 (1985).
14. Previous simulations (*9*) have shown that at these conditions methane, the third component of the ice layer, transforms into saturated hydrocarbons of heavier molecular weight that do not contribute to the electrical conductivity.
15. P. Focher, G. L. Chiarotti, M. Bernasconi, E. Tosatti, M. Parrinello, *Europhys. Lett.* **36**, 345 (1994); M. Bernasconi *et al.*, *J. Phys. Chem. Solids* **56**, 510 (1995).
16. We used a gradient correction to the local-density approximation (*26*) that accurately describes the hydrogen bonding (*27*). Norm-conserving pseudopotentials (*28*) and an integration time step of 0.075 fs were used. The electronic wavefunctions were expanded in plane waves up to a kinetic energy cutoff of 70 Ry and assumed to have the same periodicity of the simulation cell.
17. P. V. Hobbs, *Ice Physics* (Clarendon, Oxford, 1974).
18. K. R. Hirsch and W. B. Holzapfel, *Phys. Lett.* **101**, 142 (1984); Ph. Pruzan *et al.*, *J. Chem. Phys.* **99**, 9842 (1993); K. Aoki *et al.*, *Phys. Rev. Lett.* **76**, 784 (1996); A. F. Goncharov *et al.*, *Science* **273**, 218 (1996). The existence of ice X, first inferred from spectroscopy but not yet observed directly, has been confirmed by ab initio molecular dynamics (*10*), which yield a transition pressure of 102 GPa (72 GPa) by treating the proton as a classical (quantum) particle.
19. J. S. Loveday *et al.*, *Phys. Rev. Lett.* **76**, 74 (1996).
20. W. B. Hubbard and J. J. MacFarlane, *J. Geophys. Res.* **85**, 225 (1980).
21. Uncertainties on phase boundaries are related to the limited simulation times and cell sizes. They are estimated from the simulated hysteresis loop.
22. The isentropes of Uranus and Neptune are believed to be similar (*8*, *29*).
23. The ionic conductivity has been computed from the proton diffusion coefficient, the effective charge, and the Nerst-Einstein relation. The proton effective charge is $\sim+e$ as obtained from the calculation of the change in polarization associated to diffusion by the Berry-phase formalism of (*30*).
24. Although we have not performed simulations above 300 GPa, where we found a metallization temperature for water of 7000 K, the metallization temperature is expected to decrease with pressure (as it does in going from 150 to 300 GPa).
25. W. B. Hubbard, *Science* **275**, 1279 (1997).
26. A. D. Becke, *Phys. Rev.* **A 38**, 3098 (1988); C. Lee, W. Yang, R. G. Parr, *ibid.* **B 37**, 785 (1988).
27. M. Sprik, J. Hütter, M. Parrinello, *J. Chem. Phys.* **105**, 1142 (1996).
28. N. Troullier and J. L. Martins, *Phys. Rev.* **B 43**, 1993 (1991).
29. M. Podolak, A. Weizman, M. Morley, *Planet. Space Sci.* **43**, 1517 (1995).
30. R. D. King-Smith and D. Vanderbilt, *Phys. Rev.* **B 47**, 1651 (1993).
31. R. J. Hemley *et al.*, *Nature* **330**, 737 (1987).
32. F. Datchi, P. Loubeyre, R. LeToullec, *Rev. High Pressure Sci. Technol.* **7**, 778 (1998).
33. A. C. Mitchell and W. J. Nellis, *J. Chem. Phys.* **76**, 6273 (1982).
34. Calculations for water at 300 K and 66 GPa give ρ = 2.86 g/cm^3, in agreement with x-ray data (2.83 g/cm^3) (*31*).

35. We acknowledge partial support from Istituto Nazionale per La Fisica della Materia and Ministero dell' Universitá e della Ricerca Scientifica e Technologica.

12 August 1998; accepted 17 November 1998

Liquid Morphologies on Structured Surfaces: From Microchannels to Microchips

Hartmut Gau, Stephan Herminghaus, Peter Lenz, Reinhard Lipowsky*

Liquid microchannels on structured surfaces are built up using a wettability pattern consisting of hydrophilic stripes on a hydrophobic substrate. These channels undergo a shape instability at a certain amount of adsorbed volume, from a homogeneous state with a spatially constant cross section to a state with a single bulge. This instability is quite different from the classical Rayleigh Plateau instability and represents a bifurcation between two different morphologies of constant mean curvature. The bulge state can be used to construct channel networks that could be used as fluid microchips or microreactors.

Structured surfaces that exhibit lateral patterns of varying wettability can be produced by different techniques, such as microcontact printing (*1, 2*), vapor deposition (*3*), and photolithography (*4, 5*). It appears very promising to use such patterns as templates for three-dimensional (3D) structures that extend into adjacent soft matter phases.

In the present study, we created a pattern with a high wettability contrast for water. In order to obtain stripes that are as hydrophilic as possible, we generated the wettable regions by thermal vapor deposition of MgF_2 onto a hydrophobic silicone rubber or a thiolated gold substrate through appropriate masks. Both substrates exhibited the same hydrophobicity, as measured by the corresponding contact angles. The masks consisted of grids that are commercially available for electron microscopy and yielded arrays of parallel stripes with a width of a few tens of micrometers, separated by hydrophobic stripes of the same width. The thickness of the MgF_2 layer was typically 20 nm. The pattern was exposed to water vapor at a humidity of 40%. When cooled to the temperature 5°C below the dew point, the water condenses on the wettable hydrophilic regions, producing liquid microchannels.

If one deposits a small amount of water on the hydrophilic MgF_2 stripes, the microchannels are homogeneous and are shaped as cylinder segments with a constant cross section (Fig. 1A). As more and more water is adsorbed onto these channels, their volume grows until they undergo a sudden transition to a morphologically different state, and each channel then exhibits a single bulge with a characteristic shape (Fig. 1B).

Experimentally, we used optical microscopy in order to observe the contours of the

H. Gau and S. Herminghaus, Max-Planck-Institute (MPI) of Colloids and Interfaces, Rudower Chaussee 5, D-12489, Berlin-Adlershof, Germany. P. Lenz and R. Lipowsky, MPI of Colloids and Interfaces, Kantstrasse 55, D-14513 Teltow-Seehof, Germany.

*To whom correspondence should be addressed.

Superionic and Metallic States of Water and Ammonia at Giant Planet Conditions

C. Cavazzoni, G. L. Chiarotti, S. Scandolo, E. Tosatti, M. Bernasconi and M. Parrinello (January 1, 1999)

Science **283** (5398), 44-46. [doi: 10.1126/science.283.5398.44]

Editor's Summary

Science (print ISSN 0036-8075; online ISSN 1095-9203) is published weekly, except the last week in December, by the American Association for the Advancement of Science, 1200 New York Avenue NW, Washington, DC 20005.